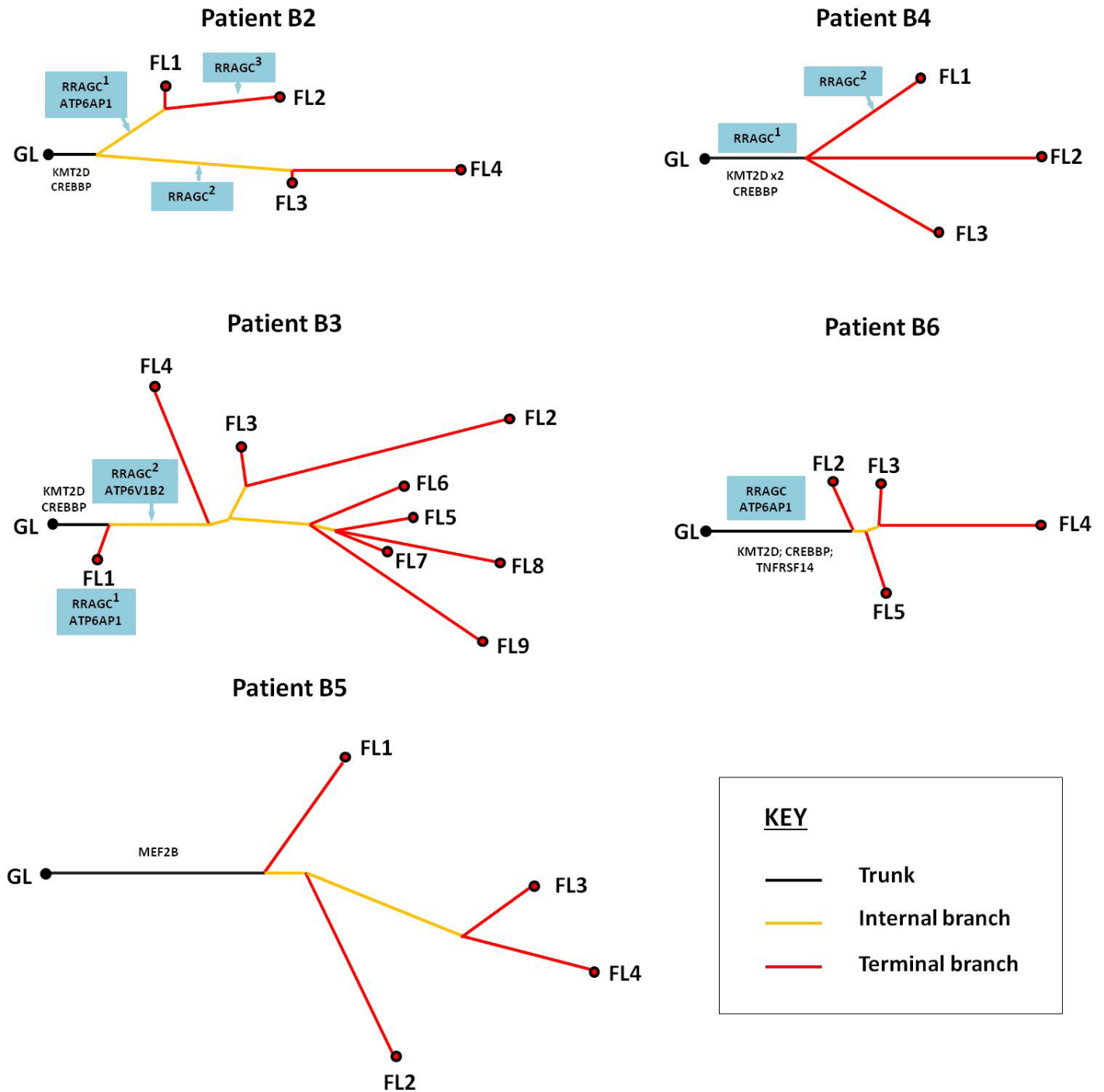


Supplementary Figure 1

Clinical timeline for the discovery WES cases.

This illustrates the timeline of the disease events during the clinical course of each patient's disease, further indicating the available samples that were sequenced in this study.

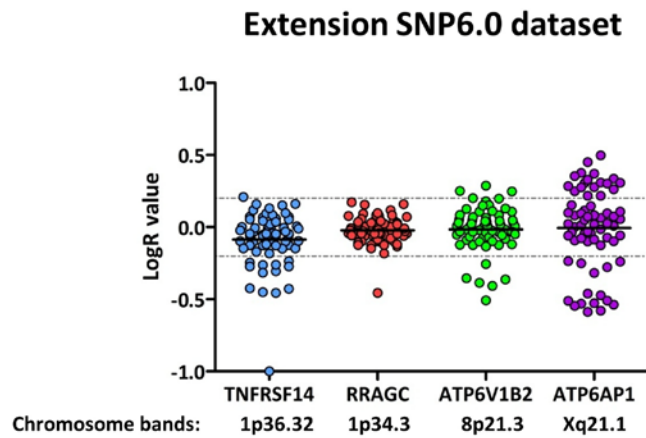
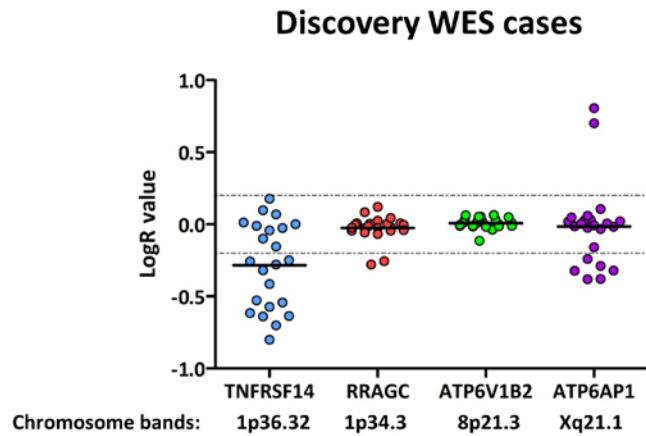


Supplementary Figure 2

Phylogenetic reconstruction demonstrating the clonal evolution history of each of the five WES cases.

In each case, a phylogenetic tree was constructed using the somatic nonsynonymous variants detected in the WES analyses. All trees are rooted at the germline (GL) sequence, with the trunk of the tree representing variants shared by all the tumor biopsies, depicting a common ancestral origin. Internal branches indicate variants that are shared by more than one subsequent progressed or relapse tumor, and the terminal branches illustrate variants that are unique or phase specific to that biopsy alone. Early initiating genes are shown on the trunk of the tree. Novel genes identified in this study (*RRAGC*, *ATP6V1B2* and *ATP6AP1*) are also illustrated. For

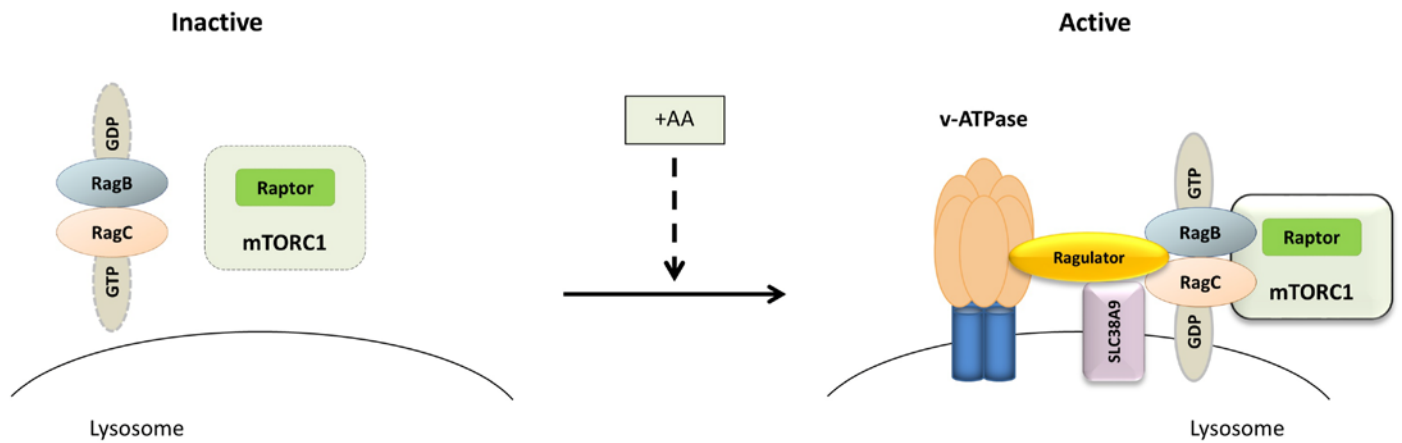
RRAGC mutations, the superscript numbers in cases B2, B3 and B4 indicate the different *RRAGC* mutations identified in those individual biopsies.



Supplementary Figure 3

Copy number of *RRAGC* as compared to other gene loci.

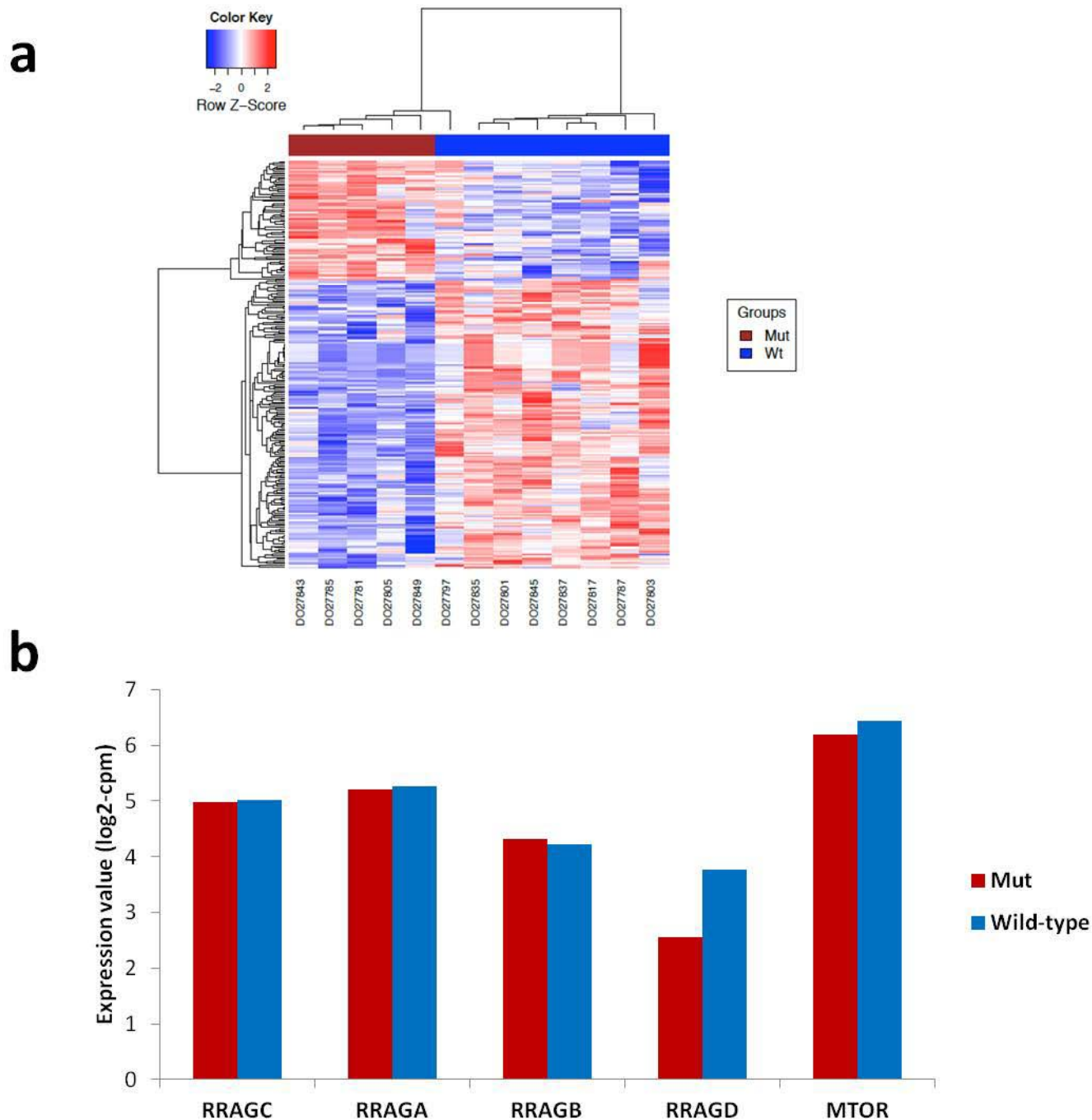
The top panel shows the log R values for each of the gene loci indicated from all 24 samples from the five WES cases, and the bottom panel shows the log R values from our previously published SNP6.0 data set comprising 29 different follicular lymphoma samples and corresponding paired transformed follicular lymphoma. The gene locus for *TNFRSF14*, 1p36.32, was chosen as a reference locus as it is commonly subject to frequent copy number deletions in follicular lymphoma. The horizontal dashed line indicates the log R value of -0.2 , with values below this measure indicative of deletions and those above 0.2 indicative of gains, as reported previously³.



Supplementary Figure 4

Model of components of the amino acid-induced mTORC1 pathway.

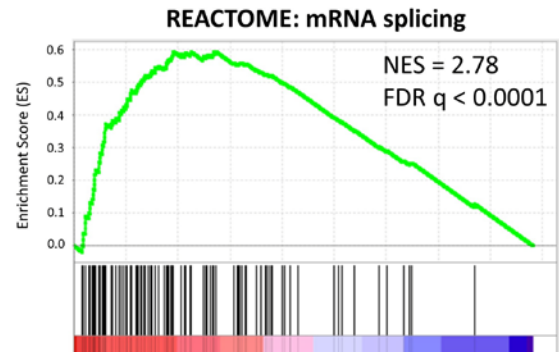
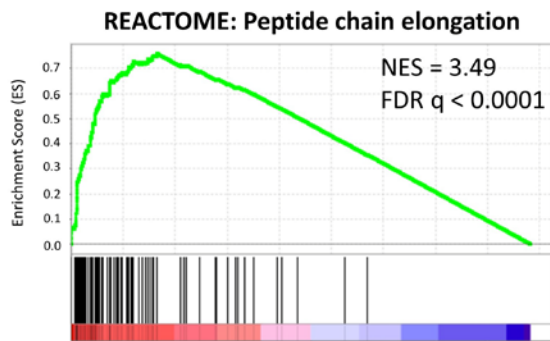
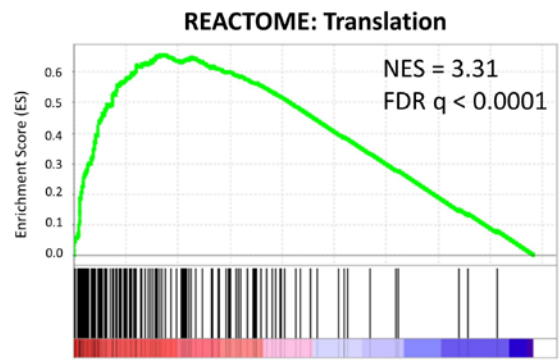
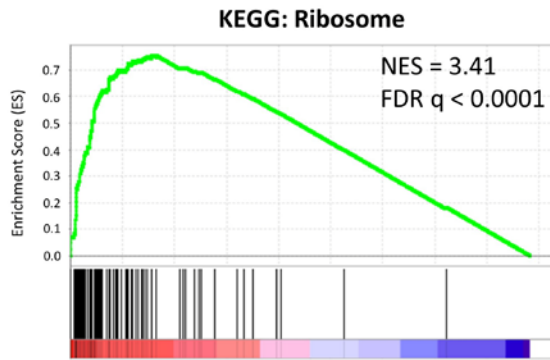
At low amino acid levels (left), the Rag heterodimer (RagB-RagC) is in a nucleotide-bound configuration incompatible for the recruitment and activation of mTORC1. In the presence of sufficient amino acids (right), a supercomplex comprising the v-ATPase, Ragulator, SLC38A9 and the Rag GTPase heterodimer translocates to the lysosomal surface. This changes the Rag heterodimer into its active form with RagB being GTP bound and RagC being GDP bound, resulting in the recruitment and activation of mTORC1.



Supplementary Figure 5

Differential gene expression between *RRAGC*-mutated and wild-type follicular lymphoma cases.

(a) Heat map from the unsupervised hierarchical clustering of genes that are differentially expressed in *RRAGC*-mutated (red bar; $n = 5$) and wild-type (blue bar; $n = 8$) tumors. This consisted of 75 upregulated and 182 downregulated genes, selected on the basis of a double threshold of raw P value < 0.01 and absolute fold change > 2 . (b) Mean gene expression values for *RRAGC*, *MTOR* and the other Rag GTPases. No difference in expression was noted between *RRAGC*-mutated and wild-type tumors. Expression values were measured using voom log₂-cpm (read count per million reads).

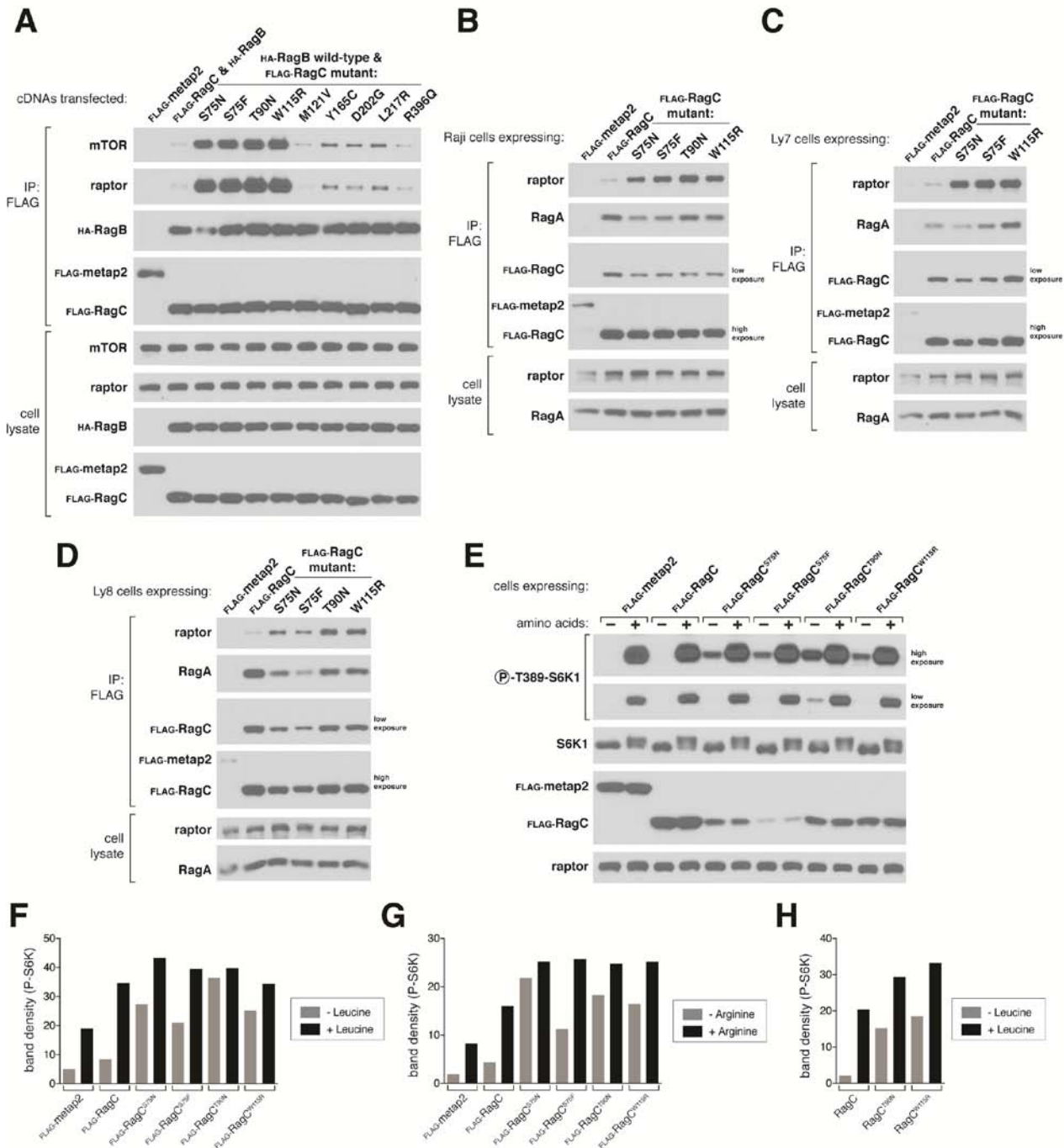


Supplementary Figure 6

Representative GSEA plots.

GSEA of gene expression data derived from RNA-seq of five *RRAGC*-mutated versus eight *RRAGC*-wild type cases. This showed significant enrichment for gene sets in several processes involved in translation and cell cycle regulation, which were upregulated in the *RRAGC*-mutated tumors as compared to wild-type tumors. Hits displayed below the graph show where the members of the gene set appear in the ranked list of genes. FDR q values and further gene sets are fully listed in **Supplementary Table 10**.

Supp. Figure 7



Supplementary Figure 7

Recurrent follicular lymphoma RagC mutants activate the mTORC1 pathway.

(a) Follicular lymphoma RagC mutants (RagC^{S75F}, RagC^{S75N}, RagC^{T90N} and RagC^{W115R}) dramatically increase mTORC1 binding (mTOR and raptor), whereas *RRAGC* mutations identified in solid cancers (p.M121V, p.Y165C, p.D202G, p.L217R and p.R396Q) did not coimmunoprecipitate mTORC1 as strongly. Anti-FLAG immunoprecipitates were collected and analyzed as in **Figure 3a**. (b) All four RagC mutants coimmunoprecipitate more raptor than wild-type RagC in Raji cells. Anti-FLAG immunoprecipitates from Raji cells stably

expressing the indicated proteins were collected and analyzed as in **Figure 3a**. (c) Three RagC mutants (RagC^{S75N}, RagC^{S75F} and RagC^{W115R}) coimmunoprecipitate more raptor than wild-type RagC when overexpressed in OCI-Ly7 cells. Anti-FLAG immunoprecipitates from OCI-Ly7 cells stably expressing the indicated proteins were collected and analyzed as in **Figure 3a**. (d) Four RagC mutants increase raptor binding over wild-type RagC in OCI-Ly8 cells. Anti-FLAG immunoprecipitates from Ly8 cells stably expressing the indicated proteins were collected and analyzed as in **Figure 3a**. (e) Stable overexpression of RagC^{S75N}, RagC^{S75F}, RagC^{T90N} and RagC^{W115R} renders the cells partially insensitive to full amino acid deprivation. HEK293T cells that stably expressed the indicated proteins were starved of amino acids for 50 min and restimulated with amino acids for 10 min. The cell lysates were analyzed as in **Figure 3b**. (f) Quantification of the amount of phosphorylated S6K1 in **Figure 3c**, under leucine starvation or starvation followed by restimulation in HEK293T cells stably expressing the indicated proteins. (g) Quantification of the amount of phosphorylated S6K1 in **Figure 3d**, under arginine starvation or starvation followed by restimulation in HEK293T cells stably expressing the indicated proteins. (h) Quantification of the amount of phosphorylated S6K1 in **Figure 3e**, under leucine starvation or starvation followed by restimulation in Karpas-422 cells stably expressing the indicated proteins.

Supplementary Table 1 Sequencing metrics for the five WES cases

	Germline (GL)	Tumor
Mean number of reads* per sample (M)	103.7	119.9
Mean sequenced nucleotides for captured regions (Gb)	6.4	7.2
Mean coverage (X)	127.0	142.7
% of target bases covered by at least 10 reads	98.2%	97.3%

*Including both forward and reverse strands

Supplementary Table 2 Clinical features and treatment details for the five discovery cases analyzed by whole exome sequencing

Patient ID	Age at diagnosis (years)	Sex	Stage at diagnosis	t(14;18)	FL grade at diagnosis	Disease event	Treatment
B2	55	F	4	Y	1	Diagnosis	FL1 (Apr 02): Expectant management
						Progression	FL2 (Dec 04): Chl
						Relapse	FL3 (Dec 10): R-CHOP + R maintenance
						Relapse	FL4 (Feb 12): Bendamustine + GA101
B3	36	F	4	Y	1	Diagnosis	FL1 (Dec 93): Expectant management
						Progression	FL2 (Dec 97): Chl + Bexxar
						Relapse	FL3 (Dec 98): FMD then CHOP
						Progression	FL4 (Aug 00): Expectant management
						Relapse	FL5 (Apr 02): Velcade
						Relapse	FL6 (Oct 02): Expectant management
						Progression	FL7 (Aug 03): Post-radiotherapy
						Relapse	FL8 (Oct 06): Chl + Rituximab
B4	37	M	Unk	Y	1	Diagnosis	FL1 (Mar 89): Chl
						Relapse	FL2 (May 91): Chl
						Relapse	FL3 (Jan 93): Surgical excision, followed by autologous SCT
B5	46	M	4	Y	2	Diagnosis	FL1 (May 88): Expectant management
						Progression	FL2 (Jan 91): Chl, then cyclophosphamide
						Progression	FL3 (Sept 97): Expectant management
						Progression	FL4 (Dec 03): Rituximab + anti-CD22
B6	50	F	3	Y	1	Diagnosis	FL1 (Feb 97): Expectant management
						Progression	No biopsy (Aug 01): Chl
						Relapse	FL2 (May 02): CHOP
						Relapse	FL3 (May 03): BEAM-R, then fludarabine
						Relapse	FL4 (Oct 03): Etoposide, cytarabine followed by vincristine and methotrexate
Relapse	FL5 (Feb 07): Velcade + Rituximab, followed by RIC-SCT						

Chl: chlorambucil; CHOP: cyclophosphamide, doxorubicin, vincristine, prednisolone; R: rituximab; GA101: obinutuzumab; FMD: fludarabine, mitoxantrone, dexamethasone; IFRT: involved field radiotherapy; Unk: unknown; BEAM: carmustine, etoposide, cytarabine, melphalan; RIC-SCT: reduced intensity conditioning stem cell transplantation